Journal of Visualization, Vol. 2, No. 1 (1999) 25-30

Visualization of Vortex Breakdown Structures

Dedicated to Professor Dr.-Ing., Dr.techn.E.h. Jürgen Zierep on the occasion of his 70 th birthday.

Bühler, K.*

* University of Applied Science (Fachhochschule), Badstrasse 24, D-77652 Offenburg, Germany.

Received 19 January 1999.
Revised 20 April 1999.

***Abstract*:** Shapes and structures of vortex breakdown phenomena in rotating fluids are visualized. We investigate the flow in a cylindrical container and in a cone between two spherical surfaces. The primary swirling flow is induced by the rotating upper disk in the cylindrical case and by the lower boundary in the spherical case. The upper surface can be fixed with a no slip condition or can be a stress-free surface. Depending on these boundary conditions and on the Reynolds number novel structures of recirculation zones are realized. Experiments are done to visualize the topological structure of the flow and to determine their existence range as function of the geometry and rotation rate. A comparison between the experimental and theoretical approach shows a good agreement in respect to the topological structures of the flows.

***Keywords*:** vortex breakdown, rotating fluids, recirculation zones, confined geometries, fixed and stress-free boundaries, flow visualization.

1. Introduction

Vortex breakdown phenomena occur in open and confined flow situations. The development of recirculation flow structures is often investigated in cylindrical geometries. In this work we studied a general case, where the fluid is contained in a cone between two spherical surfaces. The geometry and the boundary conditions strongly influence the flow pattern and therefore also the momentum and energy transport behaviour. In our investigation we are concentrated on flow structures with local recirculation zones. In a number of theoretical and experimental studies it has been shown, that local recirculation zones are an important phenomenon in nature and technology. This fact is shown in many theoretical and experimental investigations (Benjamin, 1992; Escudier, 1984; Lugt and Abboud, 1987).

The studies are based on a cylindrical geometry. In spherical gap flows such recirculation zones can be found under special conditions as it is shown by Bar-Yoseph et al.(1990). Investigations of these phenomenon in conical geometries within a spherical coordinate system are first described in Bühler (1995).

2. Cylindrical Geometry

A principle sketch of the cylindrical box experiment is shown in Fig. 1. The geometry is given by the height H and the radius R of the upper rotating disk. The angular velocity of the disk is ω. The box is filled by a viscous fluid of water-glycerin mixture with ν as kinematic viscosity. The problem is characterized by the two nondimensional parameters H/R of the geometry and the Reynolds number $Re = R^2\omega/\nu$ for the dynamic of the flow.

The circumferential velocity component induced by the upper rotating disk is superimposed by a meridional flow with radial and axial velocity components. Hence, the actual flow results in a threedimensional velocity field.

The visualized flow structure with a recirculation zone is shown in Fig. 1. Two different food colours, namely green and red are introduced in the center of the bottom as well as through a hole which is in a small distance of the center. A stagnation point is formed on the vertical axis followed by the rotationally symmetric recirculation zone. Behind this flow region the streamsurfaces sligthly diverge. The excentrically introduced red colour clearly shows the spiral character of the flow. The existence range for this single recirculation zone is described in Escudier (1984).

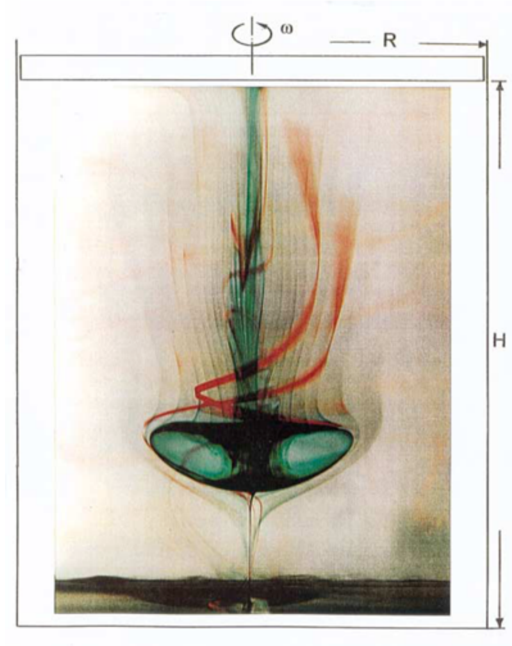

Fig. 1. Vortex breakdown in a cylindrical container with rotating upper disk, visualization by different colours, height to radius ratio $H/R = 1.7$, Reynolds number $Re = R^2\omega/\nu = 1800$.

3. Spherical Geometry

3.1 Experimental Apparatus

A graphical illustration of the conical sector between two spherical surfaces in principal is shown in Fig. 2. The boundaries of the flow region are identical with the spherical coordinate system.

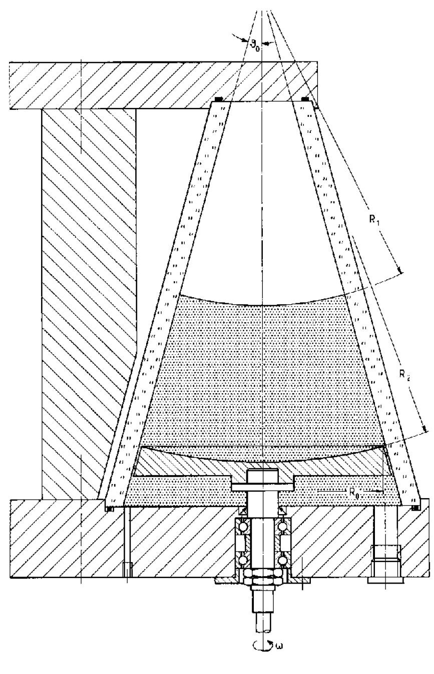

Fig. 2. Principle sketch of the flow geometry with boundaries of a spherical coordinate system, half open angle $\theta_0 = 15^{\circ}$, R_2 =300 mm, R_0 = 77.65 mm, the radius R_1 can be varied by the fluid height.

The geometry is then given by the two radii R_1 and R_2 of the inner and outer spherical surface and the half cone angle θ_0. The kinematic viscosity ν characterizes the test fluid. The rotation is given by the angular velocity ω. With the radius R_0 defined as follows:

$$R_0 = R_2 \cdot \sin\theta_0$$

the problem is characterized by the three nondimensional parameters:

$$Re_0 = \frac{R_0^2 \cdot \omega}{\nu}, \qquad \alpha = \frac{R_2}{R_1}, \qquad \theta_0.$$

In addition we need the different initial and boundary conditions.

The test fluid fills the conical transparent perspex box. The top and bottom boundaries are spherically curved. The half opening angle is $\theta_0 = 15^\circ$. The lower surface is curved by an radius R_2 = 300 mm and rotates about the vertical axes. The largest distance to the rotation axes is R_0 = 77.65 mm. The upper radius R_1 can be varied and is given by the parameter α. The test fluid is a water-glycerin mixture with a kinematic viscosity of $\nu = 5 \times 10^{-5}$ m²/s. Coloured ink is introduced on the top of the test section to visualize the flow structure. The varation of a spherical curved plate on the top allows the variation of the fluid height. In the case of a free upper surface stress-free boundary conditions are realized. The rotation speed is measured to control the angular velocity whereas the temperature of the test fluid regulates the kinematic viscosity.

3.2 Experimental Results

The observed flow structure depends strongly on the height of the fluid and on the upper boundary condition. We start with the fixed upper surface. Figure 3 shows the result for the geometry parameter $\alpha = 2.0$ and a Reynolds number $Re_0 = 3600$. The recirculation zone follows the stagnation point on the axis. The flow outside this recirculation zone moves from top to bottom along a spirally formed streamsurface. The fluid height, characterized by the geometry parameter α, has a strong influence on the structure of the recirculation zone. The stagnation point is closer to the upper fixed surface and the radial extension is larger with decreasing α. There is a strongly dependence of these structures on the Reynolds number, which is described in detail in the previous paper by Bühler (1995).

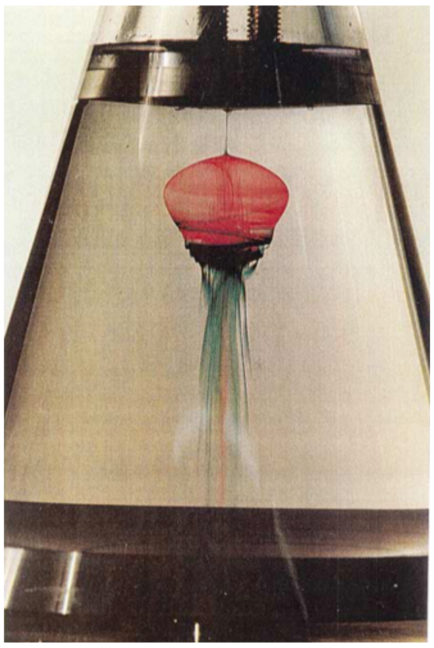

Fig. 3. Flow structure with recirculation zone, experimental result with fixed upper and rotating lower surface, $\alpha = 2.0$, $Re_0 = 3600$.

In Fig. 4 the case with a stress-free upper boundary is shown. This boundary condition is realized by a free surface of the test fluid. In some cases a stagnation point is formed on the axis between the upper free and lower fixed surface. Decreasing the fluid height and increasing the Reynolds number leads to recirculation structures touching the free surface. Instead of a stagnation point a circular stagnation line occurs as can be seen in Fig. 4. The spiralling character of the swirling motion is visible in this picture. The Reynolds number dependence of the flow structure is shown in Fig. 5. The fluid height is fixed with $\alpha = 1.48$ and the Reynolds number is increased. Starting from rest, a recirculation zone is formed on the axis with two stagnation points after the Reynolds number exceeds a critical value. The recirculation zone increases

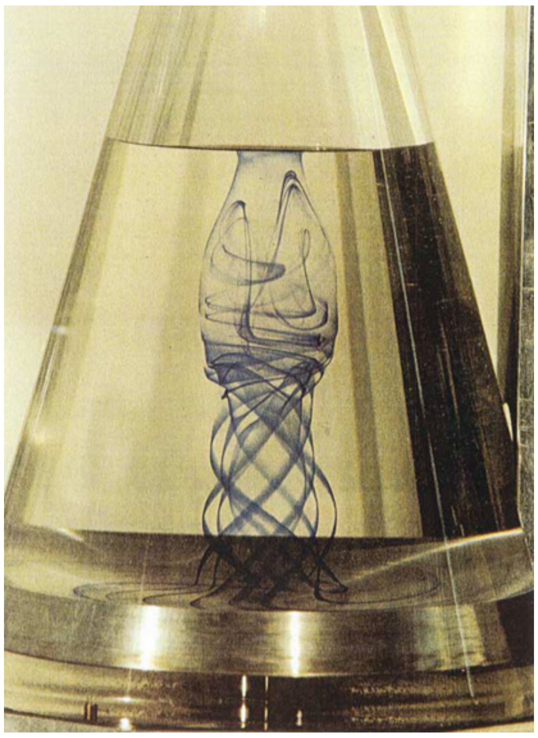

Fig. 4. Flow structure with recirculation zone, experimental result with stress-free upper surface, $\alpha = 2.0$, $Re_0 = 2260$.

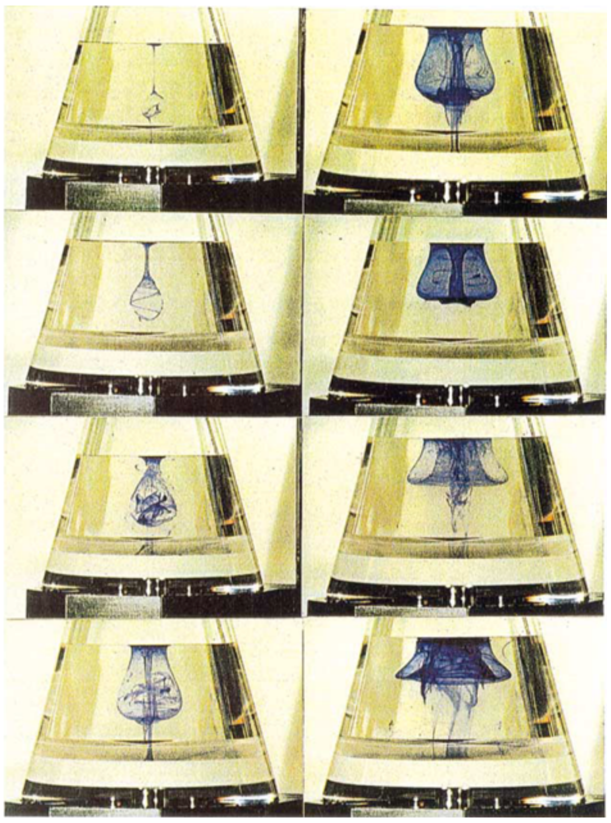

Fig. 5. Recirculation flow structures with stress-free upper surfaces for different Reynolds numbers, $Re_0 = 760, 900, 1100, 1220, 2060, 2500, 2760, 2900$; $\alpha = 1.48$.

in size with increasing Reynolds number and the stagnation point moves toward the free surface. Then the structure of the recirculation zone changes their form and a circular stagnation ring develops on the surface. A further increase of the Reynolds number leads to a second circular stagnation line at the surface, which is visualized in Fig. 5. The corresponding numerical results are described in Bühler (1995, 1998).

4. Comparison between Experiment and Theory

The investigations concern both experimental and theoretical aspects. The numerical simulation of the rotational symmetric flow is based on a finite difference method using the streamfunction-vorticity-formulation. Details of the numerical method for solving the Navier-Stokes equations in spherical coordinates can be found in the comprehensive papers by Bühler (1985, 1995). In Fig. 6 experimental results are shown on the top and the corresponding numerical results at the bottom.

The numerical solutions are visualized by lines of constant streamfunction in the meridional plane of the spherical sector. The upper boundary is a stress-free surface. The Reynolds number on the left is $Re_0 = 3000$ and 4000 on the right. The size of the recirculation zone increases with the Reynolds number. There is a good agreement between the experiment and the numerical result concerning the global structure of the flow pattern in the meridional plane.

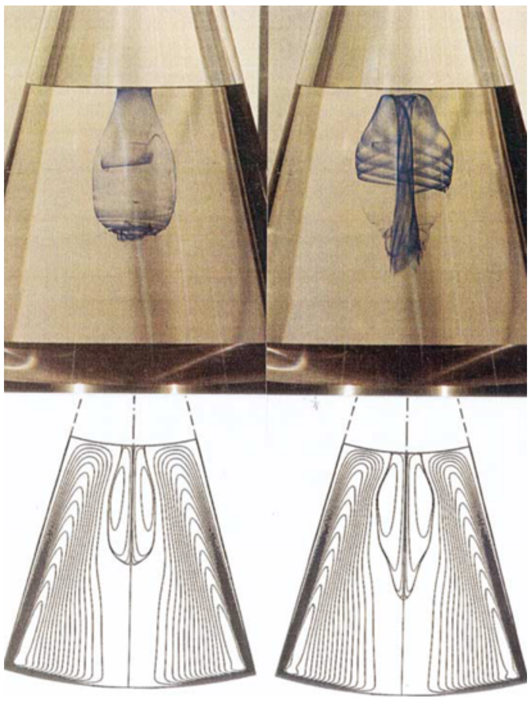

Fig. 6. Recirculation flow structures with stress-free upper surfaces for different Reynolds numbers, $Re_0 = 3000$ on the left and $Re_0 = 4000$ on the right, geometry parameter $\alpha = 2.0$, comparison between experiment and theory.

5. Conclusion

The topological flow structures are strongly depending on the container geometry. The visualization of the flows exhibits interesting new details of vortex breakdown phenomena. Novel flow patterns are obtained as function of different boundary conditions and Reynolds numbers. The comparison between experimental observations and numerical simulations shows a good agreement with respect to the topological structure of the recirculation zones.

References

Bar-Yoseph, P., Solan, A. and Roesner, K. G., Numerical simulation and experimental verification of cavity flows, Lecture Notes in Mathematics, (1990), Springer-Verlag, Berlin, pp. 229-235.

Benjamin, T. B., Theory of the vortex breakdown phenomenon, J. Fluid Mech., (1992), 14, pp. 593-629.

Bühler, K., Strömungsmechanische Instabilitäten im Kugelspalt, (1985), Fortschrittberichte Reihe 7, Düsseldorf VDI.

Bühler, K., Vortex breakdown phenomena in rotating fluids, Proc. ASME FED-Vol.218 Experimental and numerical flow visualization, (1995), pp. 45-51.

Bühler, K., Visualization of flow structures in rotating fluids, Proceedings of the 8th International Symposium on Flow Visualization (Sorrento), (1998), paper 79, pp. 1-11.
Escudier, M. P., Observations of the flow produced in a cylindrical container by a rotating end wall, Experiments in Fluids 2, (1984), pp. 189-196.
Lugt, H. J. and Abboud, M., Axisymmetric vortex breakdown with and without temperature effects in a container with a rotating lid, J. Fluid Mech., (1987), 179, pp. 179-200.

Author's Profile

Karl Bühler : He received his Ing.grad. degree in mechanical engineering in 1971 from the University of Applied Science Offenburg and his Dipl.-Ing. degree in mechanical engineering in 1975 from the University of Karlsruhe. He finished his Dr.-Ing. degree in 1979 applying optical measuring techniques in heat transfer problems. Then his research in rotating fluids leads to the Dr.-Ing.habil. degree for fluid mechanics in 1985. After that he teaches various aspects of fluid mechanics at the University Karlsruhe in the Institute of Professor Dr.-Ing., Dr.techn.E.h. Jürgen Zierep. In 1991 he takes up his current position as Professor at the University of Applied Science Offenburg. His research interests concern the areas: Instabilities in viscous heat conducting media, rotating fluids, vortex flow phenomena, behaviour of solutions of the Navier-Stokes equations, optical measuring techniques and flow visualization.